scientific reports

Check for updates

OPEN

Neuroglobin regulates autophagy through mTORC1/RAPTOR/ULK-1 pathway in human neuroblastoma cells

Valeria Manganelli[1,8], Michele Costanzo[2,3,8], Daniela Caissutti[1], Illari Salvatori[1,4], Niccolò Candelise[5], Emiliano Montalesi[1], Giovanna De Simone[6], Alberto Ferri[4,7], Tina Garofalo[1], Maurizio Sorice[1], Margherita Ruoppolo[2,3], Agostina Longo[1,9] & Roberta Misasi[1,9]✉

Neuroglobin (NGB) is a hexacoordinated hemeprotein mainly expressed in neurons. Following its upregulation and mitochondrial localization, NGB plays a pro-survival role against neuronal stress. Previously, we built a stable NGB-FLAG-overexpressing neuroblastoma cell line and showed that NGB promotes autophagy and localizes in autophagolysosomes. Here we studied the interactome of NGB-FLAG cells to identify novel autophagy-related NGB-binding partners and investigate how its upregulation could induce autophagy. LC3-II and p62 levels as well as mTORC1 activity were analyzed to evaluate autophagy in NGB-FLAG cells. NGB interactors were identified by affinity purification-mass spectrometry and protein-protein interaction network analysis and validated by immunoprecipitation. The increase of LC3-II and decrease of p62 in NGB-FLAG compared to control confirmed that NGB overexpression promotes autophagy. Interactome analysis identified the Regulatory associated protein of mTOR (RPTOR) as one of 134 putative NGB interactors, further validated by immunoprecipitation. NGB overexpression also determined a consistent increment of RPTOR phosphorylation at Ser792 which is required for mTORC1 inhibition, then confirmed by lower levels of phospho-mTOR and phospho-ULK1 in NGB-FLAG compared to control. Collectively, our data suggests that NGB is a positive regulator of autophagy. Through association with RPTOR, NGB may promote its activation and inhibit mTORC1 repressive activity on autophagy initiation.

Keywords Neuroglobin, Raptor, Autophagy, Neuroblastoma cells

Abbreviations

AMPK	AMP-dependent protein kinase
AP-MS	Affinity purification-mass spectrometry
CBL E3	ubiquitin-protein ligase CBL
co-IP	Co-immunoprecipitation
CRAP	Contaminant repository for affinity purification
CREBBP	CREB-binding protein
Cyt	Cytochrome
DDA	Data-dependent acquisition
GFP	Green fluorescent protein
GNAI1	Guanine nucleotide-binding protein G(i) subunit alpha-1
GNAI2	Guanine nucleotide-binding protein G(i) subunit alpha-2

[1]Department of Experimental Medicine, Sapienza University of Rome, Rome 00161, Italy. [2]Department of Molecular Medicine and Medical Biotechnology, University of Naples Federico II, Naples 80131, Italy. [3]CEINGE–Biotecnologie Avanzate Franco Salvatore S.C.Ar.L, Naples 80145, Italy. [4]Santa Lucia Foundation IRCCS, Rome 00179, Italy. [5]National Center for Drug Research and Evaluation, Italian National Institute of Health (ISS), Rome 00161, Italy. [6]Department of Sciences, University of Rome "Roma Tre", Rome 00146, Italy. [7]Institute of Translational Pharmacology (IFT), National Research Council (CNR), Rome 00133, Italy. [8]Valeria Manganelli and Michele Costanzo contributed equally to this work. [9]These authors jointly supervised this work: Agostina Longo and Roberta Misasi. ✉email: roberta.misasi@uniroma1.it

HRP	Horseradish peroxidase
HTT	Huntingtin
IP	Immunoprecipitation
LAMP1	Lysosome-associated membrane glycoprotein 1
LC-MS/MS	Liquid chromatography-tandem mass spectrometry
LFQ	Label-free quantification
LR	Likelihood ratio
MAMs	Mitochondria-associated endoplasmic reticulum membranes
MAP1LC3/LC3	Microtubule-associated proteins 1A/1B light chain 3
MAP2K7	Dual specificity mitogen-activated protein kinase kinase 7
mTOR	Mammalian target of rapamycin
mTORC1	mTOR complex 1
NGB	Neuroglobin
PASEF	Parallel accumulation serial fragmentation
PPI	Protein-protein interaction
PVDF	Polyvinylidene difluoride
Raptor/RPTOR	Regulatory-associated protein of mTOR
SDS-PAGE	Sodium dodecyl sulfate-polyacrylamide gel electrophoresis
p62/SQSTM1	Sequestosome1
SS18L1	Calcium-responsive transactivator
TBC1D5	TBC1 domain family member 5
TBS	Tris buffer saline
TSBT	TBS containing 0,05% v/v Tween 20
ULK1	Unc-51-like autophagy activating kinase 1
UQCRQ	Cytochrome b-c1 complex subunit 8
VDAC	Voltage-dependent anion channel

Neuroglobin (NGB) is a 17 kDa monomeric hexa-coordinated heme protein belonging to the globin family. NGB is a globular metalloprotein which, like all globins, has a tertiary structure characterized by six or four α-helices that form a sandwich around a heme group[1,2]. While in Hemoglobin and Myoglobin proteins the heme-Fe is pentacoordinate, the heme-iron of NGB is hexacoordinated by four pyrrole N atoms within the heme plane. As a globin, the main physiological functions of NGB are binding of O_2, scavenging and detoxification of reactive species[2–5].

Since its discovery, NGB has been characterized as a globin with preferential expression in the brain, where it plays an active role as a sensor of oxidative stress and acts as a cytoprotective factor against neurodegeneration, so much so that it can be considered part of the neuroprotective endogenous pathways[6]. The protective role of neuroglobin in different cell lines was shown to be related to numerous molecular NGB interactors and signaling pathways in which the globin may play a role[7]. It has been suggested that NGB is a stress-inducible protein and its overexpression and mitochondrial localization could provide a compensatory response to injury, playing a role against neurodegeneration[8,9]. Furthermore, it has been demonstrated that NGB functions as a metabolic regulator and enhances cellular anabolism[10] and that its overexpression is responsible for the increased energy metabolism in neuroblastoma cells. Several differentially regulated proteins involved in oxidative phosphorylation and integral mitochondrial proteins related to energy metabolism have been identified from proteomic analysis[3,11,12]. Indeed, overexpression of NGB increased mitochondrial ATP production, improved bioenergetic metabolism and increased oxygen consumption rate. These data converge on an active role of NGB in the adaptive response to stress in neuroblastoma cells.

Since stressing conditions induce a relocation of endogenous human neuroglobin NGB to mitochondria[13], the neuroprotective role of NGB is probably related to a synergic mechanism which involves mitochondria functions, decreasing the secretion of reactive oxygen species and nitric oxide and inhibiting the intrinsic pathway of cell death[3,9]. Moreover, we have previously demonstrated that NGB neuroprotection upon 1-methyl-4-phenylpyridinium ion (MPP+) treatment, is achieved only through interaction with the associated mitochondrial lipid raft complexes[9]. Studies of protein–protein interaction (PPI) have identified, among NGB-binding partners, the Voltage-dependent anion channel (VDAC), a subunit of mitochondrial complex III, and cytochrome (Cyt) *c*, suggesting that NGB can establish a physical interaction with mitochondrial proteins[7].

Limited information is currently available on cellular functions, including architecture, regulation, metabolism, and signaling of NGB interactors[7].

Moreover, due to its low expression, detection of NGB interactors appear to be puzzling. To this end, protein-protein interactions (PPI) analyses may aid to the understanding of NGB physiological functions[14,15]. In our previous work we have proposed autophagy as a further mechanism through which NGB may exert its protective role[11].

Autophagy is a highly conserved cytoprotective process whereby cytoplasmic contents are sequestered, transported via double-membrane autophagosomes to lysosomes, and degraded[16,17]. Autophagy ensures the release of metabolic substrates to cells satisfying their energy demands during stress and supporting cell growth and survival[18]. This process allows cells to alleviate various types of cellular stress[19]. In particular, our previous results demonstrated a role for NGB overexpressed in neuroblastoma cells in the induction of autophagy. In fact, we demonstrated a clear molecular interaction between NGB and a complex of two key molecules involved in autophagolysosome formation, light chain 3-II of microtubule-associated proteins 1 A/1B (LC3-II) and lysosome-associated membrane glycoprotein 1 (LAMP1)[11]. Hence, the involvement of NGB with the autophagic machinery could represent one of the pathways to prevent cell death associated with stress conditions.

The mammalian target of rapamycin (mTOR) is now recognized as the master regulator of autophagy. Although mTOR was first shown to negatively regulate autophagy by inhibiting the induction step, recent studies showed its involvement beyond this initial step[20]. Regulatory-associated protein of mTOR (RPTOR, henceforth referred to as Raptor) is a key element in mTOR complex 1 (mTORC1)[21,22]. In nutrient-rich conditions, activated-mTORC1 associates with the Unc-51-like autophagy activating kinase 1 (ULK1) complex via Raptor, leading to inhibition of autophagic process[23]. Since AMP-dependent protein kinase (AMPK) negatively regulates mTORC1, it is expected to positively regulate autophagy by inhibiting mTORC1. Under nutrient or growth factor-deprived or hypoxic conditions, AMPK is activated, associates with the ULK1-mTORC1 complex and leads to 14-3-3 isoforms binding to Raptor[24]. Phosphorylation of Raptor at Ser792 by AMPK inhibits mTORC1 activity, causing translocation of ULK1 to the isolation membrane at the endoplasmic reticulum, where autophagy is initiated.

This study is aimed to identify the molecular interactors of NGB, using proteomic, bioinformatic and co-immunoprecipitation (co-IP) analysis. In particular, we focused on the identification of molecule(s) involved in the neuroprotective role of NGB and its effect in the regulation of the autophagic process.

Results

Effect of NGB upregulation on autophagy induction

In our previous study, we showed a specific involvement of NGB in the formation of autolysosomes during the autophagic process, through its close association with LAMP1[11]. LAMP1 is a structural protein of lysosomes/late endosomes, used as a confirmatory marker of autophagic flux.

In this work, we first analyzed the impact of NGB overexpression on autophagy levels in SH-SY5Y cells. With this aim, we employed western blot analysis using anti-MAP1LC3/LC3 or anti- Sequestosome1 (p62/SQSTM1) antibodies, indicative of autophagy activation[11]. Indeed, p62/SQSTM1 functions as a selective autophagy receptor that captures ubiquitinated proteins and sequesters them into autophagosome vesicles through its interaction with LC3. Additionally, given that p62/SQSTM1 is a substrate for autophagic degradation, its breakdown can serve as an indicator of autophagic clearance.

The analysis revealed an increase of LC3-II levels together with a significant decrease of p62/SQSTM1 levels in NGB-overexpressing SH-SY5Y-NGB-FLAG cells as compared to control cells transfected with an empty construct (CTRL), as confirmed by densitometric analysis (Fig. 1A). In parallel, cells were also analyzed using a CytoFlex flow cytometer analysis, which confirmed a significant increase in Cyto-ID staining and a significant decrease of p62/SQSTM1 levels in NGB-overexpressing cells compared to control cells (Fig. 1B). These observations revealed that the overexpression of NGB globally enhances the autophagy process in SH-SY5Y-NGB-FLAG cells, suggesting that NGB might function as a positive regulator of autophagy. To assess autophagic flux, we inhibited autophagy with bafilomycin A1 (BafA1) and analyzed Cyto-ID staining and p62/SQSTM1 levels by flow cytometry. As expected, NGB-FLAG treated with BafA1 showed a significant increase in LC3-II (indicating autophagosome formation) along with a significant increase in p62/SQSTM1 compared to untreated cells, indicating autophagosome accumulation (Fig. S1).

Proteomic identification of NGB-interacting partners

Preliminarly, to check if the over-expressed recombinant NGB-FLAG was correctly folded with the heme we performed UV-Vis spectra of over-expressed recombinant NGB-FLAG. As reported by Li et al.[25], the oxidized form of NGB (Ngb(III)-FLAG) exhibited a strong absorption peak at 413 nm, whereas the reduced form (Ngb(II)-FLAG) displayed a Soret peak at 425 nm. In the control sample (CTRL), where NGB-FLAG was not expressed, the Soret band was absent (Fig. S2). Soret band around 415 nm is observed for proteins which hexa-coordinate ferric (Fe(III)) heme through two histidine residues[26,27]; thus these data suggest that in SH-SY5Y recombinant NGB-FLAG is overexpressed in the His-Fe-His-hexacoordinated form.

To identify the putative interactors of NGB, we used an AP-MS-based quantitative interactomic approach on NGB-interacting complexes obtained after co-IP experiments using the NGB-FLAG system as bait (Fig. 2). SH-SY5Y-NGB-FLAG cells were subjected to immunoprecipitation (IP) with anti-FLAG M2 Magnetic Beads and then analyzed by shotgun LC-MS/MS. Cells expressing a GFP-FLAG protein were analyzed using the same protocol to remove in the post-analysis non-specific interactions appearing in both the FLAG-tagged samples. Then, high-confidence NGB interactors were analyzed by bioinformatics approaches to build novel PPI networks related to NGB functions (Fig. 2).

Complexes of interacting proteins were enriched by co-IP from NGB-FLAG ($n=3$) and GFP-FLAG ($n=3$) samples (Fig. 3A) and then subjected to shotgun LC-MS/MS. The proteomic analysis of samples from independent replicates of NGB-FLAG and GFP-FLAG cells identified a total of about 4300 proteins using a timsTOF Pro mass spectrometer. To select proteins that were significantly enriched in NGB-FLAG samples (specific for NGB binding and not for FLAG or GFP affinity), we performed a LFQ-based quantitative assessment of the identified features. Within the 3518 correctly quantified proteins, we selected 134 significant species as putative NGB interactors, which were uniquely identified in NGB-FLAG samples or with an increased abundance of four-fold with respect to GFP-FLAG samples (Fig. 3B). The list of the 134 putative NGB interactors identified by quantitative interactomics is reported in Supplementary Table S1, along with their MS-identification features.

Further, putative NGB interactors were used to construct a PPI network (Fig. 3C) with relative enrichment of GO biological terms and pathways that included, for instance, calcium homeostasis, protein transport and regulation, and organelle organization (Fig. 3D). Interestingly, this network highlighted the connection of NGB with three proteins: TBC1 domain family member 5 (TBC1D5), Guanine nucleotide-binding protein G(i) subunit alpha-1 and alpha-2 (GNAI1, GNAI2). In fact, to find already known NGB interactors we additionally compared our NGB interactome with other published data. In particular, we used for this comparison *(i)* the data collected by Fiocchetti et al.[7] who explored in silico and experimentally determined NGB interactors, and *(ii)* the data provided within BioGRID database. Accordingly, the first comparison showed an overlap of three

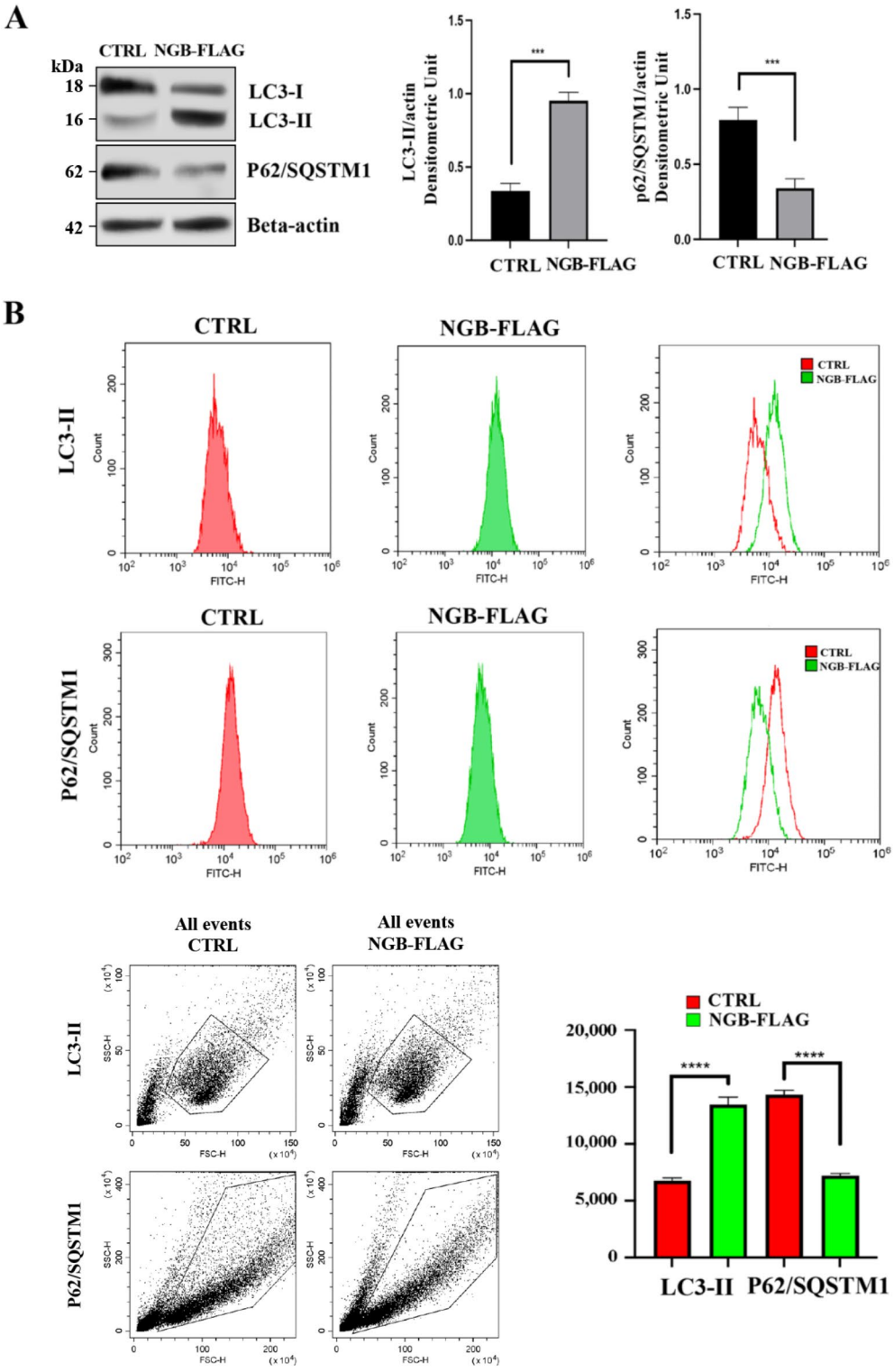

hits with our interactome, namely GNAI1, GNAI2, and Huntingtin (HTT), whereas the second one retrieved as common hits GNAI1 and TBC1D5 (Fig. 3E). This corroborated the strength of our MS data, confirming the known interaction of NGB with GNAI1, GNAI2, HTT, and TBC1D5.

To delve deeper into our MS-interactome, the first list of putative NGB interactors was refined by removing the most common contaminant species found in AP-MS-based experiments present in CRAPome, according to the specific experimental set up of this work. We obtained 61 high-confidence NGB interactors in NGB-FLAG-overexpressing SH-SY5Y cells (Table 1). These interacting partners were used to construct, from a knowledge-based data source, a refined PPI network that includes 24 interacting species, of which 16 form eight binary interactions and the other 8 are connected within a bigger net (Fig. 3F). As confirmation of the previous network, the interaction of NGB with TBC1D5 is recognized and maintained, whereas GNAI1 or GNAI2 interactions were lost as these proteins were filtered out as CRAPome contaminants. GO and pathway enrichment analysis

◀**Fig. 1**. Effect of NGB upregulation on autophagy induction. (**A**) Autophagy evaluation by Western blot analysis in NGB-overexpressing cells. SH-SY5Y cells transfected with an empty construct (CTRL) and stably transfected SH-SY5Y-NGB-FLAG cells were lysed in lysis buffer. The samples were analyzed by western blot, using rabbit anti-LC3 pAb or rabbit anti-p62/SQSTM1 mAb. Loading control was evaluated using mouse anti-Beta-Actin mAb. A representative experiment among three is shown. Bar graph on the right shows densitometric analysis. Results represent the mean ± SD from three independent experiments ($n = 3$). *** $p < 0.001$; (**B**) Autophagy evaluation by cytofluorimetric analysis in NGB-overexpressing cells. Cells were analyzed by flow cytometry after single staining with Cyto-ID autophagy detection kit to detect autophagic vesicles (autophagosomes). p62/SQSTM1 levels were analyzed by flow cytometry with rabbit anti-p62/SQSTM1 primary antibody followed by anti-rabbit Alexa Fluor 488. The gating strategy for cytometric analysis is reported in lower-left panels. Gating was performed based on forward scatter (FSC-H) and side scatter (SSC-H) values. In the lower-right panel, the values represent the mean ± SD of three separate experiments ($n = 3$). **** $p < 0.0001$. Uncropped blot images are shown in Supplementary Information file.

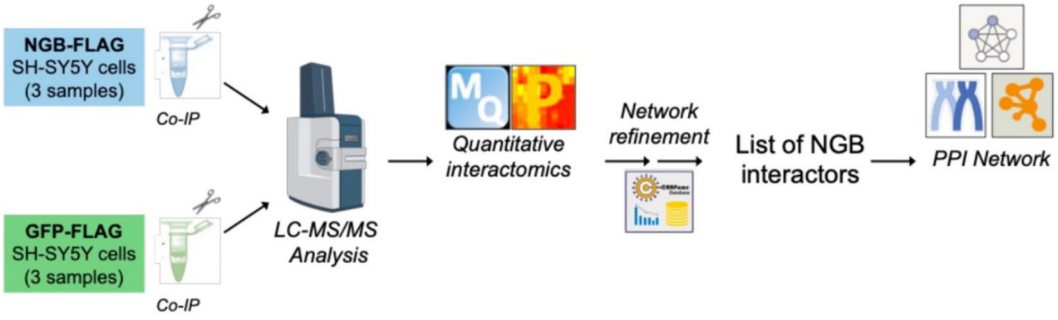

Fig. 2. Workflow of the affinity purification-mass spectrometry (AP-MS)-based approach used to identify NGB interactors in co-immunoprecipitated (co-IP) complexes. Stably transfected SH-SY5Y-NGB-FLAG cells were co-immunoprecipitated using anti-FLAG M2 Magnetic Beads. SH-SY5Y cells transfected with a Green Fluorescent Protein (GFP)-FLAG construct were used as control. Co-IP protein complexes from NGB-FLAG ($n = 3$) and GFP-FLAG ($n = 3$) were digested and analyzed by liquid chromatography-mass tandem spectrometry (LC-MS/MS). NGB-interacting partners were identified and quantified using MaxQuant and Perseus platforms. The network was refined by discarding from the preliminary MS-list of interactors those proteins identified as contaminants according to the CRAPome database. The lists of NGB interactors were analyzed by bioinformatics tools, such as STRING, Metascape and Cytoscape.

were applied to mine biological meanings connected with the extracted interactions, revealing terms involving organelle functions, and metabolic processes that included the response to hypoxia and the autophagy regulation (Fig. 3G). Many proteins of the refined NGB interactome, such as HTT, Raptor, CREB-binding protein (CREBBP), Cytochrome b-c1 complex subunit 8 (UQCRQ), Calcium-responsive transactivator (SS18L1), Dual specificity mitogen-activated protein kinase kinase 7 (MAP2K7), and E3 ubiquitin-protein ligase CBL (CBL), were also found to interact within a STRING PPI network (Fig. 3H). Interestingly, since we had previously demonstrated the involvement of NGB in the autophagic machinery[11], we focused on one identified NGB-binding protein, Raptor. First, we tried to validate in *silico* the NGB-Raptor interaction performing a PPI prediction based on structural homology and machine learning employing a non-overexpressing system. Our prediction analysis revealed that these two protein chains are not expected to interact, showing as prediction value a logLR = -2.455 (Fig. 3I). Nevertheless, since in this work we are studying a NGB-upregulated SH-SY5Y cell model, we aimed to experimentally validate NGB-Raptor interaction despite the low predicted probability of interaction.

Evidence of NGB-Raptor complex following NGB upregulation in SH-SY5Y cells

The NGB-Raptor interaction was also demonstrated by western blot analysis of immunoprecipitated complexes from SH-SY5Y-NGB-FLAG cells. To this aim, an anti-Raptor antibody was employed for IP in the SH-SY5Y CTRL or SH-SY5Y-NGB-FLAG cells. Western blot and densitometric analyses of the IP complexes revealed an increased association between NGB and Raptor in SH-SY5Y-NGB-FLAG cells as compared to CTRL cells (Fig. 4), although a weak interaction between the two proteins was discernible also in CTRL cells. No bands were detected in IPs performed with control IgG (Fig. 4). Since Raptor is a Regulatory-associated protein of mTOR[21,22], which in turn is a key regulatory of autophagy, we investigated the effect of the overexpression of NGB in mTOR-mediated signaling through the activity of Raptor. The levels of phosphorylation of Raptor at Ser792 were assessed using immunoblotting analysis. As shown in Fig. 4, the overexpression of NGB in SH-SY5Y cells resulted in increased levels of Raptor phosphorylation at Ser792 compared to control cells, as confirmed by densitometric analysis. These results strongly suggest that the overexpression of NGB could induce autophagic activation by inhibiting mTOR signaling, achieved through the phosphorylation of Raptor at Ser792. In summary, these findings imply that the upregulation of NGB may induce autophagic activation by inhibiting mTOR signaling, likely through the increase of Raptor phosphorylation.

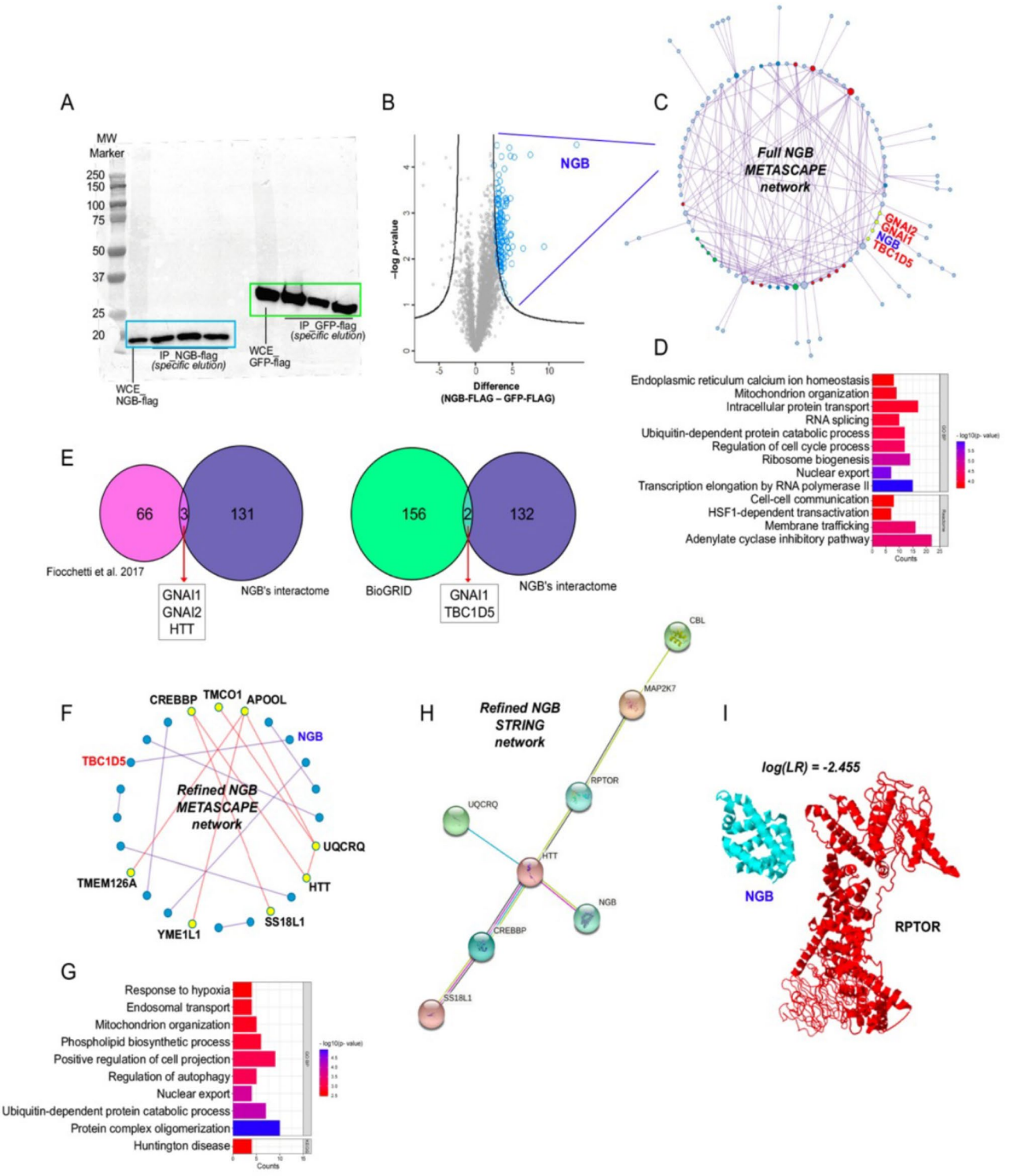

NGB overexpression induces raptor and ULK1 phosphorylation leading to autophagy induction

Given the result of the elevated phosphorylation of Raptor in NGB overexpressing cells and considering that the inhibition of mTORC1 activity through the phosphorylation of Raptor at Ser792 leads to the translocation of ULK1 in phagophore vesicles derived from the endoplasmic reticulum[28], we evaluated the mTOR signaling pathway and the phosphoserine levels of ULK1 in SH-SY5Y-NGB-FLAG cells and in the CTRL cell line. Western blot analysis, using an anti-phosphorylated (P)-Ser757-ULK1, showed a significant decrease of P-Ser757-ULK1 in SH-SY5Y-NGB-FLAG cells compared to control cells. As expected, mTOR phosphorylation was decreased in SH-SY5Y-NGB-FLAG cells compared to control cells. These results were also confirmed by densitometric analyses (Fig. 5).

◀**Fig. 3**. Analysis of the NGB interactome. (**A**) Protein complexes from NGB-FLAG ($n = 3$) and GFP-FLAG ($n = 3$) SH-SY5Y cell samples were enriched by co-IP and the specific elution of FLAG-tagged complexes by competition with FLAG peptide was assessed by SDS-PAGE. IP = immunoprecipitation, WCE = whole cell extracts. (**B**) Volcano plot shows the results of proteomic analysis of NGB-FLAG and GFP-FLAG protein complexes after identification and statistical selection of putative NGB interactors (blue circles). (**C**) Putative NGB interactors were used to construct a full PPI network with (**D**) its corresponding functional enrichment. (**E**) Venn analysis was performed to analyze the overlap between full NGB's interactome and other published NGB's interactomes data. (**F**) High-confidence NGB interactors were selected after CRAPome analysis and used to build a refined network with (**G**) its corresponding functional enrichment. (**H**) The same list of high-confidence NGB interactors was used to build a refined STRING network. (**I**) PPI prediction analysis was performed to calculate the value of predictive interaction between NGB and RPTOR. The structures of the two potential interacting proteins were reported as non-interacting chains, with a likelihood ratio (LR)= -2.455.

Together, our results provide compelling evidence for a potential mechanism by which NGB in association with Raptor regulates autophagy, specifically by targeting mTOR signaling pathway.

Discussion

There are still few studies reporting interactions between NGB and other proteins. Over the last years, by using different methodological approaches, many proteins, including cystatin C[29], prion protein[30], HTT[31], Cyt b5 and c[13,32] and thioredoxin reductase[33] were found to be associated with NGB. Finally, NGB has been reported to act as a guanine nucleotide dissociation inhibitor, binding to Gαi subunits of G proteins and thereby increasing levels of free Gβγ[34]. More recently, NGB interactomic studies have provided further evidence. On this regard, Van Acker et al. identified multiple proteins of the proteostasis machinery to bind NGB, suggesting a further possible mechanism for NGB neuroprotection. Moreover, they demonstrated that NGB interacts with proteins involved in mTOR signaling, as evidenced by its binding to key regulators under ferroptosis. These findings underscore NGB's potential role in modulating cell survival pathways, further supporting its neuroprotective functions in oxidative stress and iron-dependent cell death models[35].

Yu et al. and Haines et al. identified numerous proteins interacting with NGB, although not always validated by co-IP[36,37]. The interaction of NGB with specific molecules supports the localization of NGB in different cellular compartments and allows the identification of possible mechanisms underlying its protective effects.

Overexpression of NGB has been shown to modulate the cellular response to hypoxia, a condition that significantly impacts mTOR signaling and is intricately linked to Alzheimer's pathophysiology through autophagy impairment and energy metabolism dysregulation. Indeed, Van Acker et al. highlighted how hypoxia-induced mTOR modulation contributes to protein aggregation and synaptic dysfunction, suggesting that Ngb overexpression could play a protective role by mitigating these hypoxia-driven effects and restoring neuronal homeostasis[38]. In this work, we first analyzed the impact of NGB overexpression on autophagy levels in SH-SY5Y cells. Our results revealed that NGB might function as a positive regulator of autophagy. In fact, in NGB-overexpressing cells, we observed an increase of LC3-II levels together with a significant decrease of p62/SQSTM1 levels, as compared to SH-SY5Y cells expressing basal levels of NGB.

By most authors, NGB is considered a cytoplasmic protein[3,7–9,12]. However, some studies have shown that this globin is closely associated with mitochondrial proteins, including Cyt c1[39] and VDAC[36,40–43].

The interaction between NGB and VDAC, a porin ion channel usually localized inside the outer membrane of the mitochondrion, was first demonstrated by co-IP experiments[36,42] and subsequently validated by bioinformatic analyses[44]. The evidence of interaction between NGB and VDAC indicates the action of NGB on the direct modulation of the permeability of the outer membrane of the mitochondrion[45], a key event that leads to cell death by apoptosis[46]. Another well investigated interaction of NGB is with HTT[31]. It was suggested that HTT acts as a molecular scaffold and protein transporter[47] that allows NGB to traffic from the cytosol to mitochondria to coordinate cellular responses upon apoptotic stimuli[31,48]. NGB also interacts with plasma membrane proteins such as flotillin-1, a microdomain-associated lipid raft protein[49], which takes part in the formation of a particular type of endocytic vesicle. Moreover, NGB was shown to be enriched within lipid rafts and this interaction is crucial for NGB-mediated neuroprotection[9,50]. Interestingly, lipid rafts are not confined to the plasma membrane; in fact, these structural platforms are likely to be found in virtually all cell membranes, including endoplasmic reticulum[51], Golgi[52], nucleus[53] and mitochondria (named *raft-like* microdomains)[54–56]. Furthermore, among these platforms, mitochondria-associated endoplasmic reticulum membranes (MAMs) are characterized by the presence of specialized lipid rafts subdomains[57,58] enriched in cholesterol and gangliosides, which play a key role in regulating cell fate[59,60]. In this regard, our previous data confirmed that NGB interacts with disialoganglioside GD3, which represents a key marker of these microdomains[9], thus supporting the central role played by mitochondrial NGB.

The characterization of NGB interactors has identified crucial molecules for the neuroprotective function. Interestingly, the PPI network built with our interactomics data showed NGB connections with already known interactors[7], corroborating the strength of our MS data. At least 134 significant species detected as putative NGB interactors were found in our system. Among these, we found that Raptor is a well-represented protein, highlighting the role of NGB in the autophagic process. Further evidence of Raptor-NGB interaction is derived by our co-IP experiments. Raptor is known to be a protein associated with the regulation of mTOR[21,22]. The finding that NGB overexpression in SH-SY5Y cells resulted in increased levels of Raptor phosphorylation at Ser792 compared to control cells suggested a possible mechanism of regulation for overexpressed-NGB during

Gene names	Protein IDs	Protein names	–Log(*P*-value)	Difference*	CRAPome score#
NGB	Q9NPG2	Neuroglobin	4.489	13.9	0 / 716
KCTD2	Q14681	BTB/POZ domain-containing protein KCTD2	2.273	5.1	13 / 716
CREBBP	Q92793	CREB-binding protein	2.544	4.8	18 / 716
ADCY8	P40145	Adenylate cyclase type 8	3.313	4.8	0 / 716
QRICH1	Q2TAL8	Glutamine-rich protein 1	2.130	4.7	12 / 716
RPTOR	Q8N122	Regulatory-associated protein of mTOR	1.125	4.6	14 / 716
METTL13	Q8N6R0	Methyltransferase-like protein 13	2.389	4.4	2 / 716
TMCO1	Q9UM00	Transmembrane and coiled-coil domain-containing protein 1	2.420	4.1	30 / 716
IL1RL1	Q01638	Interleukin-1 receptor-like 1	2.482	4.0	0 / 716
COQ5	Q5HYK3	2-methoxy-6-polyprenyl-1,4-benzoquinol methylase, mitochondrial	2.808	3.9	2 / 716
KRCC1	Q9NPI7	Lysine-rich coiled-coil protein 1	1.916	3.8	0 / 716
SLC30A9	Q6PML9	Zinc transporter 9	1.400	3.8	1 / 716
SURF2	Q15527	Surfeit locus protein 2	3.153	3.8	0 / 716
MIEN1	Q9BRT3	Migration and invasion enhancer 1	2.142	3.8	3 / 716
TSSC4	Q9Y5U2	Protein TSSC4	2.829	3.7	5 / 716
WDR37	Q9Y2I8	WD repeat-containing protein 37	2.392	3.6	0 / 716
UQCRQ	O14949	Cytochrome b-c1 complex subunit 8	1.557	3.6	5 / 716
SCAMP4	Q969E2	Secretory carrier-associated membrane protein 4	2.716	3.6	2 / 716
HTT	P42858	Huntingtin	2.051	3.5	19 / 716
TMEM126A	Q9H061	Transmembrane protein 126 A	4.228	3.5	3 / 716
C17orf62	Q9BQA9	Uncharacterized protein C17orf62	1.752	3.5	0 / 716
APOOL	Q6UXV4	MICOS complex subunit MIC27	2.052	3.5	2 / 716
GPNMB	Q14956	Transmembrane glycoprotein NMB	1.922	3.4	3 / 716
KIAA1033	Q2M389	WASH complex subunit 7	2.190	3.4	17 / 716
AGPAT5	Q9NUQ2	1-acyl-sn-glycerol-3-phosphate acyltransferase epsilon	2.490	3.4	4 / 716
SOGA3	Q5TF21	Protein SOGA3	3.097	3.4	0 / 716
PIGK	Q92643	GPI-anchor transamidase	1.750	3.4	8 / 716
UBR7	Q8N806	Putative E3 ubiquitin-protein ligase UBR7	3.022	3.4	6 / 716
TBC1D5	Q92609	TBC1 domain family member 5	2.987	3.3	28 / 716
KCTD17	Q8N5Z5	BTB/POZ domain-containing protein KCTD17	1.960	3.3	10 / 716
ILK	Q13418	Integrin-linked protein kinase	3.691	3.3	10 / 716
PIGT	Q969N2	GPI transamidase component PIG-T	2.859	3.3	7 / 716
PHF23	Q9BUL5	PHD finger protein 23	2.295	3.3	1 / 716
SLC30A7	Q8NEW0	Zinc transporter 7	2.274	3.3	2 / 716
VTI1B	Q9UEU0	Vesicle transport through interaction with t-SNAREs homolog 1B	2.701	3.2	3 / 716
UBAC2	Q8NBM4	Ubiquitin-associated domain-containing protein 2	2.891	3.2	11 / 716
EPB41L5	Q9HCM4	Band 4.1-like protein 5	3.292	3.2	9 / 716
C2orf43	Q9H6V9	UPF0554 protein C2orf43	3.420	3.2	0 / 716
YME1L1	Q96TA2	ATP-dependent zinc metalloprotease YME1L1	1.925	3.2	28 / 716
SLC25A17	O43808	Peroxisomal membrane protein PMP34	1.948	3.2	5 / 716
RHBDD2	Q6NTF9	Rhomboid domain-containing protein 2	3.835	3.1	19 / 716
ARIH1	Q9Y4×5	E3 ubiquitin-protein ligase ARIH1	2.205	3.1	5 / 716
IWS1	Q96ST2	Protein IWS1 homolog	2.187	3.1	21 / 716
WBSCR22	O43709	Probable 18 S rRNA (guanine-N(7))-methyltransferase	2.704	3.1	17 / 716
SPTLC2	O15270	Serine palmitoyltransferase 2	3.549	3.1	3 / 716
NMD3	Q96D46	60 S ribosomal export protein NMD3	2.089	3.1	10 / 716
NEMF	O60524	Nuclear export mediator factor NEMF	3.202	3.1	11 / 716
OXA1L	Q15070	Mitochondrial inner membrane protein OXA1L	2.051	3.1	10 / 716
RALGAPA1	Q6GYQ0	Ral GTPase-activating protein subunit alpha-1	3.181	3.0	11 / 716
AKR1C1	Q04828	Aldo-keto reductase family 1 member C1	2.948	3.0	10 / 716
SCYL1	Q96KG9	N-terminal kinase-like protein	3.321	3.0	12 / 716
MAP2K7	O14733	Dual specificity mitogen-activated protein kinase £kinase 7	2.693	2.9	3 / 716
C2CD5	Q86YS7	C2 domain-containing protein 5	2.937	2.9	5 / 716
CBL	P22681	E3 ubiquitin-protein ligase CBL	2.762	2.9	18 / 716
DDHD2	O94830	Phospholipase DDHD2	2.845	2.9	2 / 716
YIF1A	O95070	Protein YIF1A	2.498	2.9	2 / 716
Continued					

Gene names	Protein IDs	Protein names	–Log(*P*-value)	Difference*	CRAPome score#
C18orf25	Q96B23	Uncharacterized protein C18orf25	2.378	2.9	15 / 716
PGM2	Q96G03	Phosphoglucomutase-2	2.556	2.8	25 / 716
EHD1	Q9H4M9	EH domain-containing protein 1	2.402	2.8	5 / 716
SS18L1	O75177	Calcium-responsive transactivator	2.958	2.7	17 / 716
DDA1	Q9BW61	DET1- and DDB1-associated protein 1	4.031	2.5	4 / 716

Table 1. The list of the 61 high-confidence NGB interactors identified by AP-MS. *Proteins were ordered according to decrescent values of Difference. #CRAPome score indicates a stringent high–confidence selection based on a number of deposited experiments £30/716.

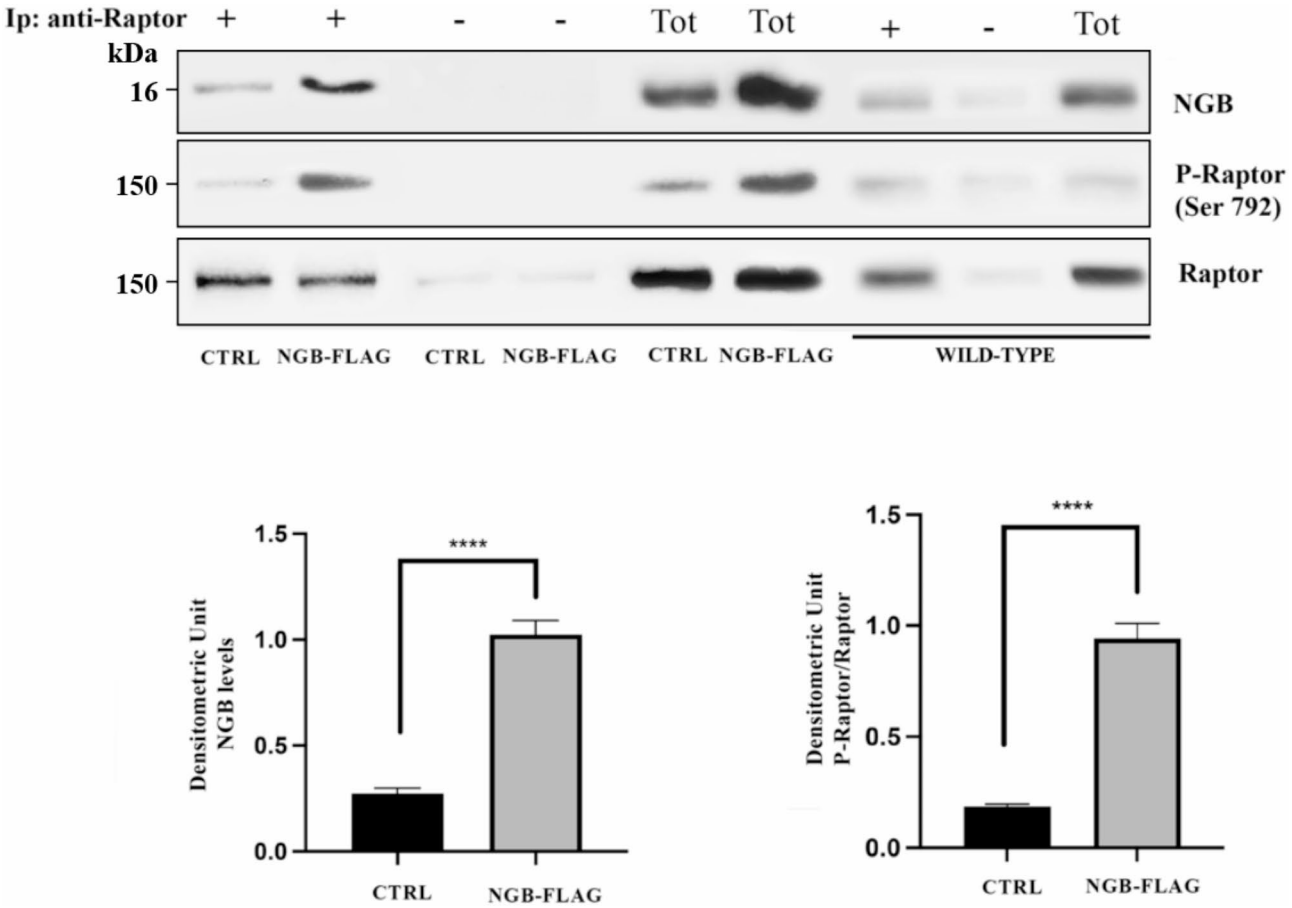

Fig. 4. Association of NGB-Raptor in SH-SY5Y cells. CTRL and stably transfected SH-SY5Y-NGB-FLAG cells were lysed in lysis buffer. The supernatant was immunoprecipitated (IP) with mouse anti-Raptor pAb plus protein G-acrylic beads. A mouse IgG isotypic control was used. IPs were analyzed by immunoblot analysis using rabbit anti-Phospho (P)-Raptor (Ser792) antibody or rabbit anti-NGB antibody. IPs were also checked by Immunoblot analysis for the presence of Raptor, using rabbit anti-Raptor mAb. The values represent the mean ± SD of three separate experiments ($n = 3$). **** $p < 0.0001$. Wild type cell line was used to validate cell systems in the experiment. Uncropped blot images are shown in Supplementary Information file.

autophagic activation. In fact, these data suggest a mechanism by which, through the phosphorylation of Raptor at Ser792, NGB inhibits mTOR signaling, consequently activating the autophagic cycle.

Overall, these findings imply that NGB might function as a positive regulator of autophagy, establishing a connection through various interactors. This insight suggests a complex network of molecular interactions in which NGB plays a pivotal role, potentially orchestrating a cascade of events that contribute to the enhancement of the autophagic process. The characterization of these interactors could provide valuable insights into the intricate mechanisms through which NGB exerts its influence on autophagy regulation.

Pharmacological regulation of the potential mechanism by which NGB influences autophagy, involving the modulation of mTOR pathways to facilitate the activation of autophagic processes, may represent a new approach in all the pathological events in which autophagy plays a role.

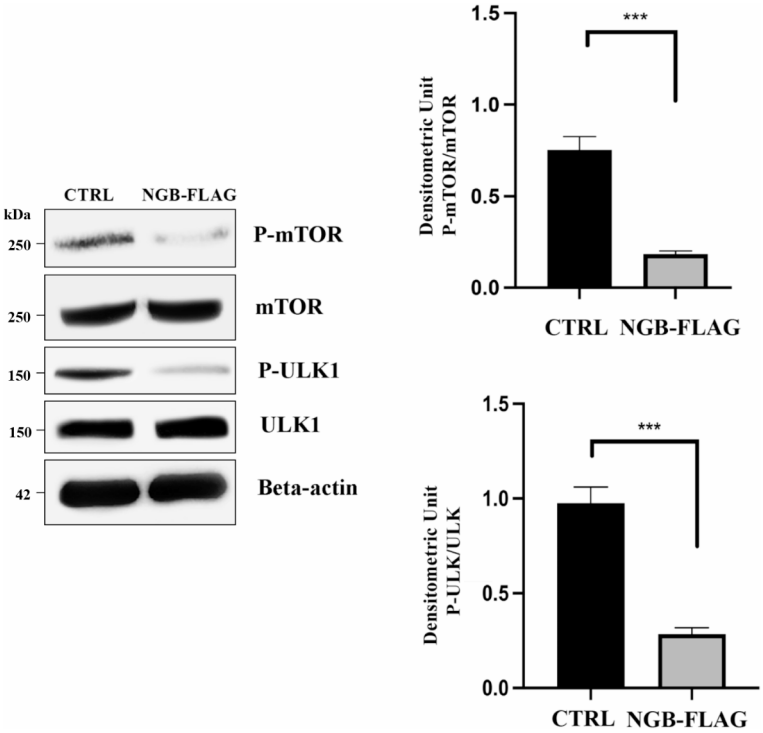

Fig. 5. NGB overexpression regulates autophagy targeting mTOR signaling pathway. CTRL and stably transfected SH-SY5Y-NGB-FLAG cells were lysed in lysis buffer. The lysates were analyzed by western blot to detect P-Ser2448-mTOR or total mTOR protein levels, using anti-P-Ser2448-mTOR pAb or anti-total mTOR pAb or P-Ser757-ULK1 or total ULK1 using anti-P- Ser757-ULK1 pAb. Loading control was evaluated using mouse anti-Beta-Actin mAb. Results represent the mean ± SD from three independent experiments ($n = 3$). *** $p < 0.001$. Uncropped blot images are shown in Supplementary Information file.

Materials and methods

Plasmid Preparation

Plasmid encoding human neuroglobin fused with 3XFLAG at C-Term (NGB-FLAG) was constructed as previously described[9]. Human NGB ORF (NCBI Reference Sequence: NM_021257.3) was subcloned by conventional PCR from NGB-pCMV6-XL5 vector (Origene Technologies, Inc., Rockville, MD, USA), using the forward primer 5′-AAAAAGATATCATGGAGCGCCCGGAGCCCGAG-3′ and the reverse primer 5′-AAAAC TCGAGCTCGCCATCCCAGCCTCGACT-3′. The resulting PCR fragment was then inserted into *EcoRV/XhoI* restriction site of pcDNA3.1-FLAG (Invitrogen, Waltham, MA, USA). Plasmid construction was evaluated by automated sequencing. The construct encoding FLAG-Tagged GFP (GFP-FLAG) was obtained by cloning GFP cDNA into pCMV3-N-FLAG plasmid (Sino Biological, Beijing, China).

Cell culture and transfection

Human neuroblastoma SH-SY5Y cell line was purchased from the American Type Culture Collection (CRL-2266, ATCC, LGC Standards S.r.l., Milan, Italy) and cultured in DMEM/F-12–Dulbecco's Modified Eagle Medium: Nutrient Mixture F-12 (D8437, Sigma-Aldrich, St. Louis, MO, USA), added with 10% fetal bovine serum (AU-S1810-500, Aurogene, Rome, Italy), 10 mg/mL streptomycin and 100 units/mL penicillin (AU-L0022-100, Aurogene, Italy), in a humified 5% CO2 incubator at 37 °C.

SH-SY5Y cell lines stably expressing human neuroglobin or GFP-FLAG were established by transfection and selection, as previously described[61]. Briefly, SH-SY5Y cells were transfected with pcDNA3.1-FLAG-NGB or with pCMV3-GFP-FLAG plasmid using Lipofectamine Plus reagent (A12621, Invitrogen), according to the manufacturer's instructions. In parallel, SH-SY5Y cells were also transfected with an empty vector as control cells (CTRL). After 3 weeks of selection with 400 µg/mL G418 (10131-027, Gibco, Waltham, Massachusetts, USA), single clones were isolated and screened based on expression level of FLAG-tagged NGB or of GFP-FLAG.

Control and stably expressing SH-SY5Y-NGB-FLAG cells were grown in complete DMEM/F-12 medium supplemented with 50 µg/mL G418.

Autophagy evaluation by Western blot

CTRL and stably transfected SH-SY5Y-NGB-FLAG cells were lysed in lysis buffer, containing 1% Triton X-100 (1610407, Bio-Rad Laboratories, Hercules, California, USA), 10 mM Tris-HCl, pH 7.5, 150 mM NaCl, 5 mM EDTA, 1 mM Na_3VO_4 (450243, Sigma-Aldrich) and protease inhibitor cocktail (P8340, Sigma-Aldrich) for 30 min at 4 °C. The lysate was centrifuged for 5 min at 1300 x g to remove nuclei and large cellular debris.

After evaluation of the protein concentration by Bradford Dye Reagent assay (Bio-Rad Laboratories), the lysate was subjected to 15% sodium-dodecyl sulfate-polyacrylamide gel electrophoresis (SDS-PAGE). The proteins were electrophoretically transferred onto polyvinylidene difluoride (PVDF) membranes (1620177, Bio-Rad Laboratories). Membranes were blocked with 5% w/v non-fat dried milk (sc-2325, Santa Cruz Biotechnology, Dallas, Texas, USA) in Tris buffer saline (1706435, Bio-Rad Laboratories) (TBS), containing 0.05% v/v Tween 20 (1706531, Bio-Rad Laboratories) (TBST) and probed with rabbit anti-LC3 pAb (NB100-2331, Novus Biologicals, Centennial, Colorado, USA), rabbit anti-SQSTM1 mAb (Cell Signaling Technology, Danvers, Massachusetts, USA), rabbit anti-P-Ser757-ULK1 pAb (6888, Cell Signaling Technology), rabbit anti-P-Ser2448-mTOR pAb (2971, Cell Signaling Technology), rabbit total ULK1 mAb (8054, Cell Signaling Technology) or rabbit anti-total mTOR mAb (2983, Cell Signaling Technology). Then, membranes were incubated with a HRP-conjugated anti-rabbit IgG secondary antibody (A1949-1VL, Sigma-Aldrich). Mouse anti-β-actin mAb (A5316, Sigma-Aldrich) and HRP-conjugated anti-mouse IgG antibody (NA931V, Sigma-Aldrich) were used to have a loading control. Immunoreactivity was assessed through the development of a chemiluminescence reaction using ChemiDoc MP Imaging System (Bio-Rad Laboratories). Clarity Western ECL Substrate chemiluminescent reagent was used for blot development (1705060, Bio-Rad Laboratories). Densitometric analysis was performed by Mac OS X (Apple Computer International, Cupertino, CA, USA), using NIH Image 1.62 software.

Autophagy evaluation by cytofluorimetric analysis

CTRL and stably transfected SH-SY5Y-NGB-FLAG cells were analyzed for autophagy evaluation by CytoFlex (Beckman Coulter, CA USA) flow cytometer after single staining with Cyto-ID detection kit (ENZ-51031-K200, Enzo Life Sciences, Exeter, UK) or with anti-p62/SQSTM1. In order to complete the data on autophagic flux, NGB-FLAG cells were also analyzed in the presence or absence of bafilomycin A1 (Baf A1, 100 nM, 120 min; B1793, Sigma-Aldrich). Cyto-ID assay was optimized using a 488 nm-excitable probe that becomes fluorescent in autophagic vesicles (autophagosomes) produced during autophagy. To detect p62/SQSTM1 levels, cells were analyzed by flow cytometry after fixation with 4% v/v formaldehyde in PBS, permeabilization with 0.1% v/v Triton X-100 in 3% w/v bovine serum albumin (A2153, Sigma-Aldrich) (BSA) in PBS for 5 min, blocking with 3% w/v BSA for 30 min and incubation with rabbit anti-p62/SQSTM1 mAb (Cell Signaling Technology) followed by anti-rabbit Alexa Fluor 488 (A11008, Invitrogen). The gating strategy for cytometric analysis is reported in lower-left panels. Gating was performed based on forward scatter (FSC-H) and side scatter (SSC-H) values. A representative experiment among three is shown. The bar graph reports the mean ± SD obtained in three independent experiments.

UV-visible absorbance spectroscopy of NGB-FLAG

60×10^6 cells of CTRL and NGB-FLAG SH-SY5Y cells were seeded in T75 flasks and cultured in complete media for 24 h. The day after, cells were collected and lysed in 200 µL of non-denaturing buffer containing 50 mM HEPES pH 8.0, 150 mM NaCl and 1% v/v Triton X-100, added with 1:100 protease inhibitor (P8340, Sigma-Aldrich). Cells were mechanically lysed on ice using high frequency sound waves for 1 min, with cycles of 10 s ON and 10 s OFF. After 10 min of centrifugation at 13,000 rpm, at 4 °C, the supernatants were collected and their UV-Vis spectra were analyzed from 380 to 480 nm by using a Lambda 365 UV-Vis spectrophotometer (Perkin Elmer, Hopkinton, MA, USA), in a 1-cm cuvette at 25 °C, with a resolution of 1.0 nm. The reduced form of Ngb(II)-FLAG (Ngb(II)-FLAG) was obtained by adding solid sodium dithionite (Sigma-Aldrich) to the Ngb(III)-FLAG sample.

Sample Preparation for affinity purification-mass spectrometry

Stably transfected SH-SY5Y-NGB-FLAG cells were used to build a PPI network of NGB using an affinity purification-mass spectrometry (AP-MS)-based interactomic approach[15]. SH-SY5Y cells transfected with a Green Fluorescent Protein (GFP)-FLAG construct were used to control the specificity of NGB interactions.

Both the cell lines in biological triplicates underwent AP-MS by co-IP using the FLAG epitope. In detail, cells were lysed in IP buffer containing 140 mM NaCl, 3 mM KCl, 25 mM Tris-HCl pH = 7.4, 1 mM EDTA, 1% Triton X-100, 10% glycerol, plus protease inhibitor cocktail (05892970001, Roche, Basel, Switzerland) at 4 °C on rotating wheel for 30 min followed by centrifugation 14,000 × *g* at 4 °C to collect supernatants. After a pre-cleaning step, protein extracts were added to anti-FLAG M2 Magnetic Beads (M8823, Sigma-Aldrich) and incubated O/N at 4 °C on rotating wheel. The day after, the beads were collected with a magnetic bar to discard the supernatant (the unbound material) and were washed eight times with IP buffer containing low (140 mM) or high (150 mM) NaCl concentrations. First, a specific elution of co-IP NGB-FLAG- and GFP-FLAG-complexes was performed per competition using the 3X FLAG peptide (F4799, Sigma-Aldrich), which was incubated with the beads for 3 h at 4 °C on rotating wheel. The supernatants containing the protein complexes were collected and used for MS or western blot analysis. Then, a second non-specific elution was carried out to check that the first elution occurred correctly. For this step, the beads were incubated in 2X Laemmli buffer for 5 min at 99 °C and then used for western blot analysis.

Digestion of Immunoprecipitated complexes and shotgun liquid chromatography-tandem mass spectrometry

Protein complexes were tryptically digested using suspension trapping (S-Trap, Prod#: C02-micro-80, ≤ 100 µg) microcolumns (Protifi, Huntington, CA, USA) as previously described[62,63]. Briefly, 10 µg of each IP protein sample were added with a final concentration of 5% SDS, reduced with 10 mM TCEP, alkylated with 40 mM IAA (iodoacetamide) for 30 min at RT, and phosphoric acid (final 2.5%) was used to completely denature proteins and trap them efficiently. Proteins were added with a binding/washing buffer (100 mM TEAB in 90% aqueous methanol) and loaded onto S-Trap columns. To efficiently remove SDS, columns were washed 4 times (4000

× *g*, 30 s) using the binding/washing buffer with a 180-degree rotation of the columns between washes. Then, protein digestion was performed at 47 °C for 4 h using trypsin (Promega, Madison, WI, USA) in a ratio 1:25 with samples content. After hydrolysis, peptides were eluted and analyzed by liquid chromatography-tandem mass spectrometry (LC-MS/MS). The system used was a nanoElute HPLC (Bruker Daltonics, Germany) coupled to a timsTOF Pro mass spectrometer (Bruker Daltonics). The LC separation was performed at 250 nL/min in a packed emitter column (C18, 25 cm × 75 µm, 1.6 µm) (Ion Optics, Melbourne, Australia) using solvents A (0.1% HCOOH in water) and B (0.1% HCOOH in ACN) with the following gradient: 2 to 11% solvent B for 19 min, 11 to 16% B for 7 min, 16 to 25% B for 4 min, 25 to 80% B for 3 min, 80% B for 7 min for column washing. MS acquisitions were carried out at m/z range of 100–1700 Th using the parallel accumulation serial fragmentation (PASEF) method in data-dependent acquisition (DDA) mode. Ion mobility was set in a range from 0.85 to 1.3 V s/cm^2 (1/K0). The total cycle time and the number of PASEF MS/MS scans were 1.2 s and 6, respectively. The mass spectrometry proteomics data have been deposited to the ProteomeXchange Consortium (http://proteomecentral.proteomexchange.org) via the PRIDE partner repository[64]. Data are available on request (michele.costanzo@unina.it).

Identification and quantification of NGB interactors

NGB interactors were identified analyzing the raw (.d) MS/MS files with MaxQuant v2.0.1.0, and quantified using the Label-free quantification (LFQ) intensities based on MaxLFQ algorithm, as described[65,66]. The protein group file was then imported into Perseus v1.6.15.0 for data processing. Protein LFQ intensities were log2-transformed, a minimum of 3/3 valid values in at least one group were selected, and missing values were replaced with numbers from a random normal distribution with width of 0.3 and downshift of 1.8. Significant interactors were selected on the basis of: (i) statistical t-test significance (FDR = 0.01) between the NGB-FLAG and GFP-FLAG conditions; (ii) quantitative difference with intensities increased in the NGB-FLAG samples (s0 = 2).

Bioinformatic analysis of NGB interactome

The refinement of NGB interactome network was achieved using the CRAPome 2.0 (Contaminant Repository for Affinity Purification) database by selecting possible non-specific contaminants identified in our AP-MS experiment. This database provides a qualitative and semiquantitative description of the propensity of a protein to be a non-specific interactor in a precise experimental setting[67]. To this aim, we interrogated the CRAPome and queried all the proteins of the NGB interactome. We selected among these only high-confidence proteins according to a priori threshold, which means that an interactor is a non-contaminant if it appears in a number of AP-MS experiments lower than 30 with respect to the total of deposited experiments (716), and considering other variables such as the epitope tag, cell line, affinity approach, and affinity support used. Otherwise, possible contaminants were filtered out from the first list of MS-identified interactors.

Functional classification of discovered interactors was carried out with Metascape v3.5.20240101 [68] on the list of total significant MS-interactors, and the refined list after CRAPome analysis. This let construct PPI networks involving NGB and enrich significant Gene Ontology (GO) terms, such as Biological Processes (BP), Reactome and KEGG pathways. Cytoscape v3.9.1 was employed to model NGB networks on the basis of Metascape algorithms. Enriched terms accounting on low redundancy, high counts and high significance were plotted using SRplot platform[69].

In addition, functional PPI networks of interactomics data were annotated with STRING v11.0 [70], inputting the list of high-confidence interactors and using *homo sapiens* as taxonomy.

Finally, we used the PEPPI tool to predict protein-protein interactions of some proteins of interest. This pipeline employs protein structural homology, search through high-throughput experimental data and machine learning-based classification to build a Bayesian model that expresses a likelihood ratio (LR), i.e. the probability of (non)interaction between two species[71].

Immunoprecipitation analysis

CTRL and stably transfected SH-SY5Y-NGB-FLAG cells were lysed in cold lysis buffer containing 1% Triton X-100, 10 mM Tris-HCl pH 7.5, 150 mM NaCl, 5 mM EDTA, plus 1 mM Na_3VO_4 and protease inhibitor cocktail (P8340, Sigma-Aldrich), for 30 min at 4 °C. Cellular lysates were centrifuged for 10 min at 17,000 × *g* and supernatant proteins were collected and quantified using Bradford protein assay reagent (Bio-Rad Laboratories).

The lysates were mixed with protein G-acrylic beads (P3296, Sigma-Aldrich) for 2 h at 4 °C and washed extensively. After centrifugation (500 x g for 1 min), the supernatant was immunoprecipitated with mouse anti-Raptor mAb (sc-81537, Santa Cruz Biotechnology) plus protein G-acrylic beads. A mouse IgG isotypic control (M5284, Sigma-Aldrich) was used. The immunoprecipitates were checked by immunoblotting analysis, using rabbit anti-Raptor mAb (2280, Cell Signaling Technology).

Immunoblotting of immunoprecipitates

Immunoprecipitates, obtained as described above, were separated on 7.5% or 15% SDS-PAGE. Proteins were then transferred onto PVDF membranes (1620177, Bio-Rad Laboratories), which were subsequently blocked for 1 h at room temperature with 5% w/v non-fat dry milk (sc-2325, Santa Cruz Biotechnology) in TSBT. Then, membranes were incubated overnight at 4 °C with either rabbit anti-NGB antibody (13499-1-AP, Proteintech, Manchester, UK) or rabbit anti-Raptor antibody (2280, Cell Signaling Technology), or rabbit anti-P-Ser792-Raptor antibody (2083, Cell Signaling Technology), both diluted 1:500 in TBST. After that, membranes were quicky washed in TBST and incubated for 1 h at room temperature with HRP-conjugated anti-rabbit IgG secondary antibody (A1949-1VL, Sigma-Aldrich), diluted 1:5000 in 2.5% non-fat dry milk in TBST. Then, membranes were washed in TBST and developed using ChemiDoc MP Imaging System (Bio-Rad Laboratories).

Statistical analysis

All the statistical procedures were performed by GraphPad Prism software Inc. (San Diego, California, USA). All data reported in this paper were verified in at least 3 different experiments performed in duplicate and reported as mean ± standard deviation (SD). The *p*-values for all graphs were generated using Student's *t*-test as indicated in the figure legends; * $p < 0.05$, ** $p < 0.005$, *** $p < 0.001$, **** $p < 0.0001$.

Data availability

The datasets generated and analysed during the current study are available in the PRIDE repository, http://proteomecentral.proteomexchange.org. Data are available on request (michele.costanzo@unina.it).The data that support the findings of this study are available in the Materials and Methods, Results, and/or Supplemental Material of this article.

Received: 27 November 2024; Accepted: 21 February 2025
Published online: 04 March 2025

References

1. Burmester, T., Welch, B., Reinhardt, S. & Hankeln, T. A vertebrate globin expressed in the brain. *Nature* **407**, 520–523 (2000).
2. Burmester, T. & Hankeln, T. Function and evolution of vertebrate globins. *Acta Physiol.* **211**, 501–514 (2014).
3. Ascenzi, P. et al. Neuroglobin: from structure to function in health and disease. *Mol. Aspects Med.* **52**, 1–48 (2016).
4. Bilska-Wilkosz, A., Iciek, M., Górny, M. & Kowalczyk-Pachel, D. The role of hemoproteins: hemoglobin, myoglobin and neuroglobin in endogenous thiosulfate production processes. *Int. J. Mol. Sci.* **18**, 1315 (2017).
5. Tiso, M. et al. Human neuroglobin functions as a redox-regulated nitrite reductase. *J. Biol. Chem.* **286**, 18277–18289 (2011).
6. Guidolin, D., Tortorella, C., Marcoli, M., Maura, G. & Agnati, L. F. Neuroglobin, a factor playing for nerve cell survival. *Int. J. Mol. Sci.* **17**, 1817 (2016).
7. Fiocchetti, M., Cipolletti, M., Brandi, V., Polticelli, F. & Ascenzi, P. Neuroglobin and friends. *J. Mol. Recognit.* **30**, e2654 (2017).
8. Fiocchetti, M. et al. Neuroglobin and mitochondria: the impact on neurodegenerative diseases. *Arch. Biochem. Biophys.* **701**, 108823 (2021).
9. Garofalo, T. et al. Neuroglobin overexpression plays a pivotal role in neuroprotection through mitochondrial raft-like microdomains in neuroblastoma SK-N-BE2 cells. *Mol. Cell. Neurosci.* **88**, 167–176 (2018).
10. Cai, B. et al. Neuroglobin overexpression inhibits AMPK signaling and promotes cell anabolism. *Mol. Neurobiol.* **53**, 1254–1265 (2016).
11. Manganelli, V. et al. Overexpression of neuroglobin promotes energy metabolism and autophagy induction in human neuroblastoma SH-SY5Y cells. *Cells* **10**, 3394 (2021).
12. Singh, S., Zhuo, M., Gorgun, F. M. & Englander, E. W. Overexpressed neuroglobin raises threshold for nitric oxide-induced impairment of mitochondrial respiratory activities and stress signaling in primary cortical neurons. *Nitric Oxide*. **32**, 21–28 (2013).
13. De Marinis, E., Fiocchetti, M., Acconcia, F., Ascenzi, P. & Marino, M. Neuroglobin upregulation induced by 17β-estradiol sequesters Cytocrome C in the mitochondria preventing H_2O_2-induced apoptosis of neuroblastoma cells. *Cell. Death Dis.* **4**, e508 (2013).
14. Ngounou Wetie, A. G. et al. Protein-protein interactions: switch from classical methods to proteomics and bioinformatics-based approaches. *Cell. Mol. Life Sci.* **71**, 205–228 (2014).
15. Santorelli, L., Caterino, M. & Costanzo, M. Dynamic interactomics by Cross-Linking mass spectrometry: mapping the daily cell life in postgenomic era. *OMICS* **26**, 633–649 (2022).
16. Parzych, K. R. & Klionsky, D. J. An overview of autophagy: morphology, mechanism, and regulation. *Antioxid. Redox Signal.* **20**, 460–473 (2014).
17. Yu, L., Chen, Y. & Tooze, S. A. Autophagy pathway: cellular and molecular mechanisms. *Autophagy* **14**, 207–215 (2018).
18. Rabinowitz, J. D. & White, E. Autophagy and metabolism. *Sci. (1979).* **330**, 1344–1348 (2010).
19. Ravanan, P., Srikumar, I. F. & Talwar, P. Autophagy: the spotlight for cellular stress responses. *Life Sci.* **188**, 53–67 (2017).
20. Rabanal-Ruiz, Y., Otten, E. G. & Korolchuk, V. I. MTORC1 as the main gateway to autophagy. *Essays Biochem.* **61**, 565–584 (2017).
21. Hara, K. et al. Raptor, a binding partner of target of Rapamycin (TOR), mediates TOR action. *Cell* **110**, 177–189 (2002).
22. Kim, D. H. et al. mTOR interacts with raptor to form a nutrient-sensitive complex that signals to the cell growth machinery. *Cell* **110**, 163–175 (2002).
23. Kim, J., Kundu, M., Viollet, B. & Guan, K. L. AMPK and mTOR regulate autophagy through direct phosphorylation of Ulk1. *Nat. Cell. Biol.* **13**, 132–141 (2011).
24. Gwinn, D. M. et al. AMPK phosphorylation of raptor mediates a metabolic checkpoint. *Mol. Cell.* **30**, 214–226 (2008).
25. Li, L. et al. Expression, purification and spectra characterization of neuroglobin. *Chin. Sci. Bull.* **50**, 1708–1713 (2005).
26. Inuzuka, T. et al. Identification of crucial histidines for Heme binding in the N-terminal domain of the Heme-regulated eIF2α kinase. *J. Biol. Chem.* **279**, 6778–6782 (2004).
27. Kupke, T., Klare, J. P. & Brügger, B. Heme binding of transmembrane signaling proteins undergoing regulated intramembrane proteolysis. *Commun. Biol.* **3**, (2020).
28. Karanasios, E. et al. Autophagy initiation by ULK complex assembly on ER tubulovesicular regions marked by ATG9 vesicles. *Nat. Commun.* **7**, 12420 (2016).
29. Wakasugi, K., Nakano, T. & Morishima, I. Association of human neuroglobin with Cystatin C, a cysteine proteinase inhibitor. *Biochemistry* **43**, 5119–5125 (2004).
30. Palladino, P. et al. Neuroglobin-prion protein interaction: what's the function? *J. Pept. Sci.* **17**, 387–391 (2011).
31. Nuzzo, M. T. et al. Huntingtin PolyQ mutation impairs the 17β-Estradiol/Neuroglobin pathway devoted to neuron survival. *Mol. Neurobiol.* **54**, 6634–6646 (2017).
32. Fago, A., Mathews, A. J., Moens, L., Dewilde, S. & Brittain, T. The reaction of neuroglobin with potential redox protein partners Cytochrome b5 and Cytochrome C. *FEBS Lett.* **580**, 4884–4888 (2006).
33. Trandafir, F. et al. Neuroglobin and Cytoglobin as potential enzyme or substrate. *Gene* **398**, 103–113 (2007).
34. Wakasugi, K., Nakano, T. & Morishima, I. Oxidized human neuroglobin acts as a heterotrimeric Gα protein guanine nucleotide dissociation inhibitor. *J. Biol. Chem.* **278**, 36505–36512 (2003).
35. Van Acker, Z. P. et al. Connecting the Dots in the neuroglobin-protein interaction network of an unstressed and ferroptotic cell death neuroblastoma model. *Cells* **8**, 873 (2019).
36. Yu, Z., Liu, N., Wang, Y., Li, X. & Wang, X. Identification of neuroglobin-interacting proteins using yeast two-hybrid screening. *Neuroscience* **200**, 99–105 (2012).
37. Haines, B. A. et al. Comparative protein interactomics of neuroglobin and myoglobin. *J. Neurochem.* **123**, 192–198 (2012).
38. Van Acker, Z. P. et al. Impaired hypoxic tolerance in APP23 mice: a dysregulation of neuroprotective globin levels. *FEBS Lett.* **591**, 1321–1332 (2017).

39. Yu, Z. et al. Roles of neuroglobin binding to mitochondrial complex III subunit cytochrome c1 in Oxygen-Glucose Deprivation-Induced neurotoxicity in primary neurons. *Mol. Neurobiol.* **53**, 3249–3257 (2016).
40. Yu, Z. et al. Mitochondrial distribution of neuroglobin and its response to oxygen-glucose deprivation in primary-cultured mouse cortical neurons. *Neuroscience* **218**, 235–242 (2012).
41. Cwerman-Thibault, H. et al. Neuroglobin effectively halts vision loss in harlequin mice at an advanced stage of optic nerve degeneration. *Neurobiol. Dis.* **159**, 105483 (2021).
42. Yu, Z., Liu, N., Li, Y., Xu, J. & Wang, X. Neuroglobin overexpression inhibits oxygen-glucose deprivation-induced mitochondrial permeability transition pore opening in primary cultured mouse cortical neurons. *Neurobiol. Dis.* **56**, 95–103 (2013).
43. Fiocchetti, M., De Marinis, E., Ascenzi, P. & Marino, M. Neuroglobin and neuronal cell survival. *Biochim. Biophys. Acta Proteins Proteom.* **1834**, 1744–1749 (2013).
44. Guidolin, D. et al. Neuroglobin as a regulator of mitochondrial-dependent apoptosis: A bioinformatics analysis. *Int. J. Mol. Med.* **33**, 111–116 (2014).
45. Bayrhuber, M. et al. Structure of the human voltage-dependent anion channel. *Proc. Natl. Acad. Sci. U S A.* **105**, 15370–15375 (2008).
46. Tait, S. W. G. & Green, D. R. Mitochondria and cell death: outer membrane permeabilization and beyond. *Nat. Rev. Mol. Cell. Biol.* **11**, 621–632 (2010).
47. Saudou, F. & Humbert, S. *Biology Huntingtin Neuron* **89**, 910–926 (2016).
48. Nuzzo, M. T. et al. 17β-Estradiol modulates Huntingtin levels in rat tissues and in human neuroblastoma cell line. *Neurosci. Res.* **103**, 59–63 (2016).
49. Wakasugi, K., Nakano, T., Kitatsuji, C. & Morishima, I. Human neuroglobin interacts with flotillin-1, a lipid raft microdomain-associated protein. *Biochem. Biophys. Res. Commun.* **318**, 453–460 (2004).
50. Watanabe, S., Takahashi, N., Uchida, H. & Wakasugi, K. Human neuroglobin functions as an oxidative stress-responsive sensor for neuroprotection. *J. Biol. Chem.* **287**, 30128–30138 (2012).
51. Hayashi, T. & Su, T. P. σ-1 receptors (σ1 binding sites) form raft-like microdomains and target lipid droplets on the Endoplasmic reticulum: roles in Endoplasmic reticulum lipid compartmentalization and export. *J. Pharmacol. Exp. Ther.* **306**, 718–725 (2003).
52. Gkantiragas, I. et al. Sphingomyelin-enriched microdomains at the golgi complex. *Mol. Biol. Cell.* **12**, 1819–1833 (2001).
53. Cascianelli, G. et al. Lipid microdomains in cell nucleus. *Mol. Biol. Cell.* **19**, 5289–5295 (2008).
54. Garofalo, T. et al. Lipid microdomains contribute to apoptosis-associated modifications of mitochondria in T cells. *Cell. Death Differ.* **12**, 1378–1389 (2005).
55. Sorice, M. et al. Dynamics of mitochondrial raft-like microdomains in cell life and death. *Commun. Integr. Biol.* **5**, 217–219 (2012).
56. Alessandri, C. et al. Antiphospholipid reactivity against Cardiolipin metabolites occurring during endothelial cell apoptosis. *Arthritis Res. Ther.* **8**, (2006).
57. Montesinos, J. & Area-Gomez, E. Isolation of mitochondria-associated ER membranes. *Methods Cell. Biol.* **155**, 33–44 (2020).
58. Garofalo, T. et al. Evidence for the involvement of lipid rafts localized at the ER-mitochondria associated membranes in autophagosome formation. *Autophagy* **12**, 917–935 (2016).
59. Garofalo, T. et al. Role of mitochondrial raft-like microdomains in the regulation of cell apoptosis. *Apoptosis* **20**, 621–634 (2015).
60. Manganelli, V. et al. Raft-like lipid microdomains drive autophagy initiation via AMBRA1-ERLIN1 molecular association within MAMs. *Autophagy* **17**, 2528–2548 (2021).
61. Cozzolino, M. et al. Cysteine 111 affects aggregation and cytotoxicity of mutant Cu,Zn-superoxide dismutase associated with Familial amyotrophic lateral sclerosis. *J. Biol. Chem.* **283**, 866–874 (2008).
62. Costanzo, M. et al. Dataset of a comparative proteomics experiment in a methylmalonyl-CoA mutase knockout HEK 293 cell model. *Data Brief.* **33**, 106453 (2020).
63. Costanzo, M. et al. Proteome data of neuroblastoma cells overexpressing neuroglobin. *Data Brief.* **41**, 107843 (2022).
64. Deutsch, E. W. et al. The proteomexchange consortium at 10 years: 2023 update. *Nucleic Acids Res.* **51**, D1539–D1548 (2023).
65. Costanzo, M. et al. Methylmalonic acidemia triggers lysosomal-autophagy dysfunctions. *Cell. Biosci.* **14**, 63 (2024).
66. Ruiz-Blázquez, P. et al. Cathepsin D is essential for the degradomic shift of macrophages required to resolve liver fibrosis. *Mol. Metab.* **87**, 101989 (2024).
67. Mellacheruvu, D. et al. The CRAPome: A contaminant repository for affinity purification-mass spectrometry data. *Nat. Methods.* **10**, 730–736 (2013).
68. Zhou, Y. et al. Metascape provides a biologist-oriented resource for the analysis of systems-level datasets. *Nat. Commun.* **10**, 1523 (2019).
69. Tang, D. et al. SRplot: A free online platform for data visualization and graphing. *PLoS One.* **18**, e0294236 (2023).
70. Szklarczyk, D. et al. STRING v11: Protein-protein association networks with increased coverage, supporting functional discovery in genome-wide experimental datasets. *Nucleic Acids Res.* **47**, D607–D613 (2019).
71. Bell, E. W., Schwartz, J. H., Freddolino, P. L. & Zhang, Y. P. E. P. P. I. Whole-proteome Protein-protein interaction prediction through structure and sequence similarity, functional association, and machine learning. *J. Mol. Biol.* **434**, 167530 (2022).

Acknowledgements

This research was funded by the Italian Ministry of Education, University and Research (MIUR) PRIN 2022 (20223RXEEC) and CaRiPT Foundation giovani@ricercascientifica to R.M.; PRIN 2022 (2022APEBMY) to T.G.; PRIN 2022 (2022XL4TE9_003), PRIN-PNRR (P2022LZP9T) to M.S., co-funding of the European Union—Next Generation EU, Mission 4 Component 2 Investment 1.5, project Rome Technopole—code ECS 00000024 (CUP: B83C22002820006) to M.S.; Istituto Superiore di Sanità, Starting Grant for young researchers 2021, File CB83; CUP I83C22002190005 to N.C.

Author contributions

V. M., M. C., A. L. and R. M. conceived and designed this study; D. C., I. S. and G.D.S. performed the experiments; A. F., N. C. and E. M. performed validation and formal analysis; V. M., M. C., T. G., M. S., M. R. and R. M. wrote the original manuscript. All authors have read and agreed to the published version of the manuscript.

Declarations

Competing interests

The authors declare no competing interests.

Additional information

Supplementary Information The online version contains supplementary material available at https://doi.org/10.1038/s41598-025-91701-w.

Correspondence and requests for materials should be addressed to R.M.

Reprints and permissions information is available at www.nature.com/reprints.

Publisher's note Springer Nature remains neutral with regard to jurisdictional claims in published maps and institutional affiliations.